Journal of Medicinal Chemistry Article

J. Med. Chem. **2010,** *53,* 7441–7451 **7441**
DOI: 10.1021/jm100886h

Assessment of Structurally Diverse Philanthotoxin Analogues for Inhibitory Activity on Ionotropic Glutamate Receptor Subtypes: Discovery of Nanomolar, Nonselective, and Use-Dependent Antagonists

Sidsel Frølund,[†] Angelo Bella,[†] Anders S. Kristensen,[†] Hanne L. Ziegler,[†] Matthias Witt,[‡] Christian A. Olsen,[†,§] Kristian Strømgaard,[†] Henrik Franzyk,*[,†] and Jerzy W. Jaroszewski*[,†]

[†]*Department of Medicinal Chemistry, Faculty of Pharmaceutical Sciences, University of Copenhagen, Universitetsparken 2, DK-2100 Copenhagen, Denmark, and* [‡]*Bruker Daltonik GmbH, Fahrenheitstrasse 4, D-28359 Bremen, Germany.*
[§]*Present address: Department of Chemistry, Technical University of Denmark, Kemitorvet 207, DK-2800 Kgs. Lyngby, Denmark.*

Received July 15, 2010

An array of analogues of the wasp toxin philanthotoxin-433, in which the asymmetric polyamine moiety was exchanged for spermine and the headgroup replaced with a variety of structurally diverse moieties, was prepared using parallel solid-phase synthesis approaches. In three analogues, the spermine moiety was extended with an amino acid tail, six compounds contained an *N*-acylated cyclohexylalanine, and four analogues were based on a novel diamino acid design with systematically changed spacer length between *N*-cyclohexylcarbonyl and *N*-phenylacetyl substituents. The analogues were studied using two-electrode voltage-clamp electrophysiology employing *Xenopus laevis* oocytes expressing GluA1$_i$ AMPA or GluN1/2A NMDA receptors. Several of the analogues showed significantly increased inhibition of the GluN1/2A NMDA receptor. Thus, an analogue containing *N*-(1-naphtyl)acetyl group showed an IC_{50} value of 47 nM. For the diamino acid-based analogues, the optimal spacer length between two *N*-acyl groups was determined, resulting in an analogue with an IC_{50} value of 106 nM.

Introduction

Because of the complexity of their physiological and biochemical manifestations, disorders of the central nervous system represent a major challenge for modern medicine. At the same time, the burden of age-related neurodegenerative diseases increases worldwide in consequence of aging populations. While the etiology of neurodegenerative diseases is often unknown and the underlying mechanisms are exceedingly intricate, degeneration of isolated neurons is known to be associated with an imbalance in their neurotransmitter receptor systems. The most common cause of dementia is Alzheimer's disease,[1−3] and two types of drugs for its relief are currently in use: acetylcholine esterase (AChE[a]) inhibitors, used mainly to slow down progress during early stages of the disease, and memantine, which is prescribed in moderate to severe stages.[4] The use of AChE inhibitors, originating from the cholinergic deficit hypothesis of Alzeimer's disease, counteracts low levels of cholinergic neurotransmission by increasing the availability of acetylcholine,[5,6] whereas memantine acts on the glutamatergic system by blocking *N*-methyl-D-aspartate (NMDA) receptors. Memantine[7−10] is believed to protect neurons from glutamate excitotoxicity without affecting physiological glutamate receptor activation required for normal function of the brain. Novel modulators of ionotropic glutamate receptors are therefore of interest as potential leads for neuroactive drug development.

Analogues of philanthotoxin-433 (PhTX-433, **1**, Figure 1) constitute a group of compounds that modulate the function of pore-forming ligand-gated receptors,[11] including ionotropic glutamate receptors (iGluR). PhTX-433 (**1**) was originally isolated from the venom of a solitary wasp, *Philanthus triangulum*.[12] PhTX-433 and its analogues inhibit iGluR by an uncompetitive mechanism, i.e., they require preactivation of the receptor, after which the toxin apparently enters and binds to the ion channel region of the receptor. This mechanism of action is believed to be similar to that of memantine. However, PhTX-433 (**1**) and its more readily available and extensively studied synthetic analogue, PhTX-343 (**2**), display potent activity on both acetylcholine-gated and glutamate-gated ion channels, and their selectivity on various subtypes of iGluR still remains largely unexplored.

iGluR are classified into three main subgroups according to their preferential activation by (*RS*)-2-amino-3-(3-hydroxy-5-methylisoxazol-4-yl)propionate (AMPA), NMDA, or kainic acid, respectively. AMPA and NMDA receptors are the most abundant iGluR and are involved in more than 80% of all excitatory transmission in the central nervous system. The receptors are composed of four subunits, where the membrane-embedded domains of the four subunits form an ion channel that controls flux of cations such as Na^+, K^+, and Ca^{2+} in response to binding of glutamate.[13−15] AMPA receptors are homomeric or heteromeric assemblies of four different subunits,

*To whom correspondence should be addressed. Phone: +45 35336372. Fax: +45 35336041. E-mail: jj@farma.ku.dk.

[a] Abbreviations: AChE, acetylcholine esterase; Adm, adamantyl; AMPA, (*RS*)-2-amino-3-(3-hydroxy-5-methylisoxazol-4-yl)propionate; BAL, backbone amide linker; Boc, *tert*-butyloxycarbonyl; Cha, cyclohexylalanine; Dab, (*S*)-2,4-diaminobutyric acid; Dap, (*S*)-2,3-diaminopropionic acid; DIC, diisopropylcarbodiimide; Fmoc, 9-fluorenylmethoxycarbonyl; gDap, (*S*)-2-amino-4-guanidinylpropionic acid; hArg, homoarginine; HOBt, *N*-hydroxybenzotriazole; iGluR, ionotropic glutamate receptor; nAChR, nicotinic acetylcholine receptor; NMDA, *N*-methyl-D-aspartate; Pfp, pentafluorophenyl; Pyrazol(Boc)$_2$, *N*,*N*′-bis(*tert*-butyloxycarbonyl)-1-guanylpyrazol; SPS, solid-phase synthesis; Teoc, 2-(trimethylsilyl)ethyloxycarbonyl; Teoc-ONp, 2-(trimethylsilyl)ethyl *para*-nitrophenyl carbonate; TFA, trifluoroacetic acid or trifluoroacetate; TFFH, tetramethylfluoroformamidinium hexafluorophosphate; VLC, vacuum liquid chromatography.

Published on Web 09/27/2010

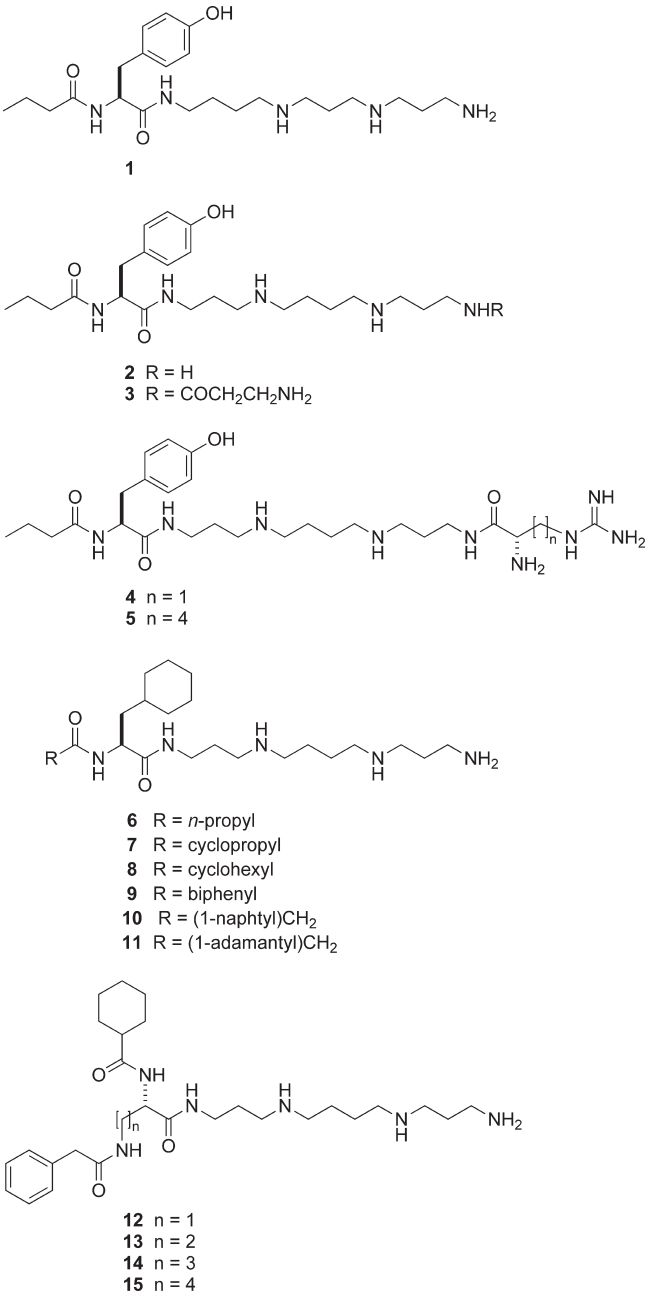

Figure 1. PhTX-433 (**1**) and analogues (**2**−**15**) investigated in the present study.

GluA1−4, whereas NMDA receptors are obligatory heteromeric assemblies of a GluN1 subunit that binds coagonist glycine and either GluN2A-D or GluN3A-B subunits.

Developments in methodology for both solid-phase synthesis (SPS)[16−24] and large-scale solution-phase[25] synthesis of philanthotoxin analogues have permitted a more rapid exploration of structure−activity relationships for these polyamine toxins. In previous studies, analogues of PhTX-343 (**2**) in which the tyrosine moiety was substituted with a cyclohexylalanine (Cha) moiety exhibited significantly enhanced inhibitory activity against embryonic muscle-type nAChR expressed in TE671 cells,[26] whereas analogues containing bulky replacements of the tyrosine moiety exhibited potencies on AMPA receptors similar to that of **2**.[27] Analogues displaying different types of amino acid tails on the polyamine moiety have also been reported.[28] Moreover, numerous analogues having polyamine chains with varying numbers and positions of amino functionalities have been prepared by solid-phase methods;[29,30] ion channel affinity of these analogues is apparently related to the number and position of positive charges present.[31,32]

In the present work, a diverse array of analogues of PhTX-343 (**2**), comprised of **3**−**15**, was prepared. All analogues contain spermine as the polyamine moiety, whereas the tyrosine component of the headgroup, present in the original toxin (**1**), was retained in **3**−**5** but was replaced with a Cha residue in analogues **6**−**11**. In compounds **12**−**15**, the entire structure of the headgroup was remodeled to give novel constructs containing *N*,*N*′-diacylated diamino acid moieties such as lysine and homologues. Because the presence of an aromatic substituent appears to be important for activity at NMDA receptors,[27,33] most of the synthesized Cha-containing analogues contain aromatic moieties in the *N*-acyl group. PhTX-343 analogues elongated with ω-amino acids (**3**−**5**) were also included in this investigation. The impact of these structural changes was evaluated at the recombinant AMPA and NMDA receptor subtypes $GluA1_i$ and GluN1/2A, respectively, expressed in *Xenopus laevis* oocytes. Two-electrode voltage-clamp electrophysiology was used to determine compound ability to inhibit agonist-induced currents at different holding potentials. Thus, the aim of this work was to explore structural requirements for potency on these two subtypes of iGluR. In addition to being drug leads, potent inhibitors of the iGluR subtypes exhibiting novel selectivity patterns are envisioned to be useful pharmacological tools.

Results and Discussion

Chemistry. SPS protocols used in this work are based on 9-fluorenylmethoxycarbonyl (Fmoc) amino group protection/deprotection strategy and on use of either pentafluorophenyl (Pfp) esters or free carboxylic acids together with common peptide coupling reagents. Compounds **2**,[25] **3**,[23] and **6**[26] were prepared as previously described. The remaining analogues of the series may be divided into three subgroups according to the SPS methodology applied for their synthesis: (i) amino acid-elongated analogues of **2** (i.e., **4** and **5**), obtained via bidirectional SPS on a backbone amide linker (BAL) resin, (ii) analogues **7**−**11**, obtained by a standard linear SPS sequence starting with the spermine moiety and followed by parallel *N*-acylation of the headgroup with different acyl groups,[16,27] and (iii) compounds **12**−**15**, prepared by a similar linear SPS sequence leading to an orthogonally protected diamino acid derivative that enabled subsequent introduction of two different *N*-acyl groups, both of which could be diversified in a parallel manner. Preparation of **4** and **5** according to (i) and synthesis of **12**−**15** according to (iii) required synthesis of guanidinylated amino acid building blocks **16** and **17** and orthogonally protected diamino acid building blocks **18**−**21**, respectively (Scheme 1). Guanidinylated building block Fmoc-hArg-(Boc_2)-OH (**16**)[36] was prepared from Fmoc-Lys(Boc)-OH using a procedure previously employed for more complex dipeptidic building blocks.[37] This involved removal of the Boc group and introduction of the protected guanidino functionality with the standard pyrazol$(Boc)_2$ reagent performed as a one-pot procedure. After purification by vacuum liquid chromatography (VLC), the product **16** was obtained in 81% yield (Scheme 1). Similarly, the derivative of (*S*)-2,3-diaminopropionic acid, compound **17**, was obtained from Boc-Dap-OH in 87% yield.

After a reaction sequence consisting of reductive amination of the BAL resin with a selectively protected spermine building block $H_2N(CH_2)_3NHBoc(CH_2)_4NHBoc(CH_2)_3NHTeoc$,[23] TFFH-mediated acylation of the resulting resin-bound secondary amine functionality with Fmoc-Tyr(Bu^t)-OH, and Fmoc deprotection, the *N*-butyryl moiety was installed using a Pfp ester[25] to give resin **22** (Scheme 2). The use of mono-Teoc-protected di-Boc-spermine rather than di-Boc-spermine, $H_2N(CH_2)_3NHBoc(CH_2)_4NHBoc(CH_2)_3NH_2$ circumvented the problem of cross-linking of the trityl linker functionalities on the resin.[23] Subsequently, removal of the Teoc group and attachment of the appropriate guanidinylated amino acid tail via standard DIC-HOBt couplings afforded resins **23** and **24**. Finally, acid cleavage (after Fmoc deprotection in the case of **24**) and purification by preparative HPLC furnished elongated philanthotoxins **4** (36% yield) and **5** (46% yield) as TFA salts.

N-Acylated Cha-PhTX analogues **7**−**11** were obtained by a modification of the previously reported solid-phase protocol,[27] again replacing the initial loading on a trityl resin of di-Boc-spermine with the loading of $H_2N(CH_2)_3NHBoc(CH_2)_4NHBoc(CH_2)_3NHTeoc$ to give resin **25**. After removal of the Teoc group, acylation with Fmoc-Cha-OH by standard DIC−HOBt coupling gave resin **26**. The latter was Fmoc-deprotected and acylated in a parallel fashion using five different carboxylic acids. Subsequent cleavage and purification furnished **7**−**11** in 42−54% yield (Scheme 3).

To obtain **12**−**15** (Scheme 4), 2-chlorotrityl resin-linked di-Boc-spermine **27**, prepared as above via a Teoc intermediate, was reacted with orthogonally protected (N^{ω}-Teoc and N^{α}-Fmoc) diamino acid building blocks **18**−**21**, prepared by treatment of appropriate starting materials shown in Scheme 1 with (2-trimethylsilyl)ethyl *p*-nitrophenyl carbonate (Teoc-ONp).[38,39] This resulted in resins **28**−**31** suited for successive introduction of two different acyl moieties. Thus, N^{α}-deprotection, condensation with cyclohexanecarboxylic acid using DIC−HOBt, N^{ω}-deprotection, and N^{ω}-acylation with the Pfp ester of phenylacetic acid completed the assembly of the frameworks **32**−**35**. Cleavage from the resin and preparative HPLC furnished the target compounds **12**−**15** in 61−78% overall yields.

Pharmacology. The inhibitory potency of the toxin analogues **3**−**15** to block receptor currents was evaluated using two-electrode voltage-clamp electrophysiology with *Xenopus laevis* oocytes expressing the flip form of the AMPA receptor subtype GluA1 ($GluA1_i$) or the NMDA receptor subunits GluN1 and GluN2A (GluN1/2A). PhTX-343 (**2**) was used as a reference compound. Initially, the inhibitory activity at a holding potential of −60 mV was measured at two concentrations of the test compounds, 0.1 and 10 μM (Figure 2). At these concentrations, **2** exhibited 59% and 95% inhibition of the $GluA1_i$ AMPA receptor, respectively. While the inhibition was essentially complete for all compounds tested at 10 μM, the

Scheme 1. Synthesis of Amino Acid Building Blocks[a]

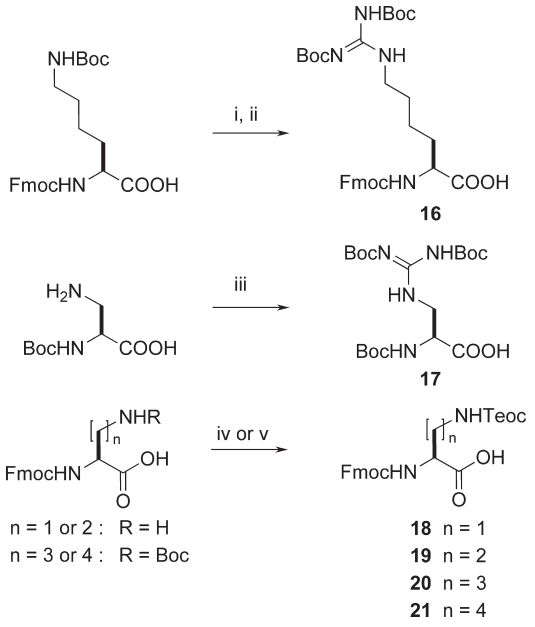

[a] Reagents: (i) TFA−CH_2Cl_2, room temperature, 1 h; (ii) pyrazol$(Boc)_2$ (1.2 equiv), *i*Pr_2EtN (5 equiv), DMF, room temperature, 16 h; (iii) pyrazol$(Boc)_2$ (1.2 equiv), *i*Pr_2EtN (2 equiv), DMF, room temperature, 16 h; (iv) Na_2CO_3 (1 equiv), Teoc-ONp (1.1 equiv), dioxane−H_2O, room temperature, 16 h; (v) TFA−CH_2Cl_2 (1:1), room temperature, 2 h then Teoc-ONp (1.9 equiv), *i*Pr_2EtN (3.3 equiv), DMF, room temperature, 16 h.

Scheme 2. SPS of PhTXs Elongated with an Amino Acid Tail[a]

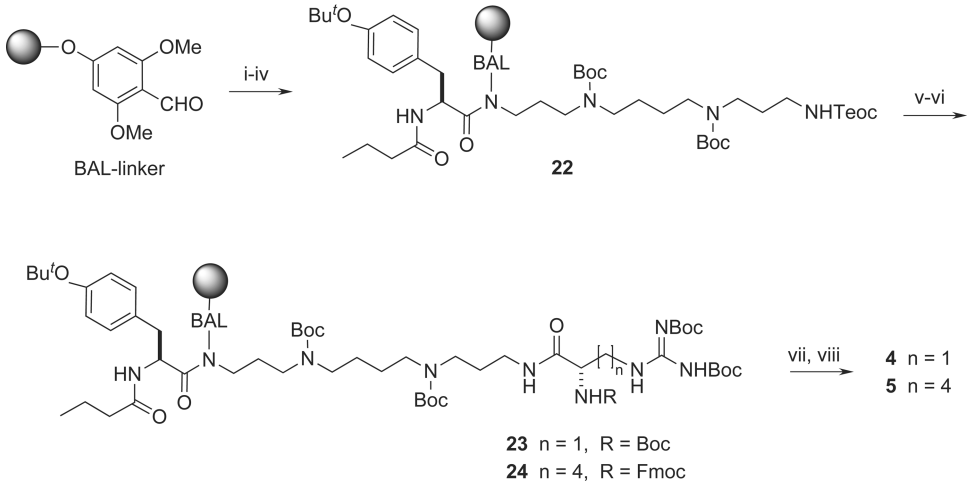

[a] Reagents: (i) $H_2N(CH_2)_3NBoc(CH_2)_4NBoc(CH_2)_3NHTeoc$ (10 equiv), $NaBH(OAc)_3$ (10 equiv), DMF−AcOH (9:1), 16 h; (ii) Fmoc-Tyr(Bu^t)-OH (4 equiv), TFFH (4 equiv), *i*Pr_2EtN (8 equiv), DMF, 3 h and then repeated for 16 h; (iii) 20% piperidine−DMF, 2 × 10 min; (iv) $C_3H_7COOPfp$ (5 equiv), *i*Pr_2EtN (5 equiv), DMF, 16 h; (v) Bu_4NF (3 equiv), DMF, 50 °C, 2 × 1 h; (vi) Fmoc-hArg(Boc_2)-OH (**16**) or Boc-gDap(Boc_2)OH (**17**) (3 equiv), HOBt (3 equiv), DIC (3 equiv), DMF, 3 h and then repeated for 16 h; (vii) only for $n = 4$, 20% piperidine−DMF, 2 × 10 min; (viii) TFA−CH_2Cl_2 (1:1), 1 h.

Scheme 3. SPS of *N*-Acylated Cha-PhTX Analogues[a]

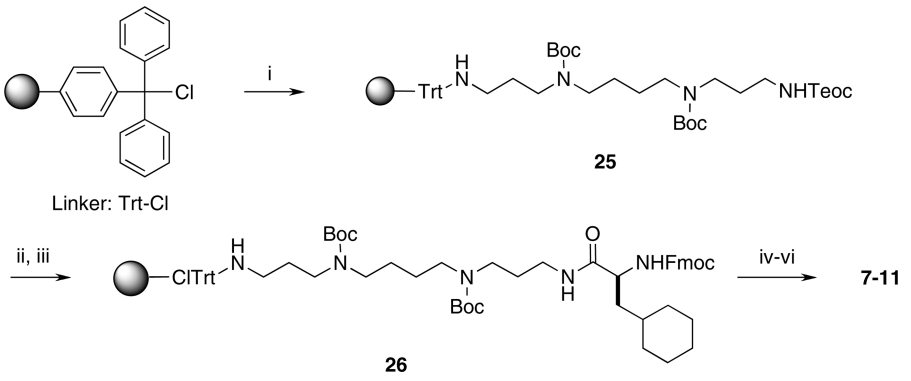

[a] Reagents: (i) $H_2N(CH_2)_3NBoc(CH_2)_4NBoc(CH_2)_3NHTeoc$ (1.0 equiv), *i*Pr_2EtN (3 equiv), CH_2Cl_2, 3 days; (ii) Bu_4NF (4 equiv), DMF, 50 °C, 1 h, then room temperature, 2 h; (iii) Fmoc-Cha-OH (3 equiv), DIC (3 equiv), HOBt (3 equiv), DMF, 16 h; (iv) 20% piperidine−DMF, 2 × 10 min; (v) Appropriate R-COOH (5 equiv), DIC (5 equiv), HOBt (5 equiv), DMF, 19 h; (vi) 50% TFA−CH_2Cl_2 (2 h).

Scheme 4. SPS of PhTX-Analogues Based on Diamino Acids[a]

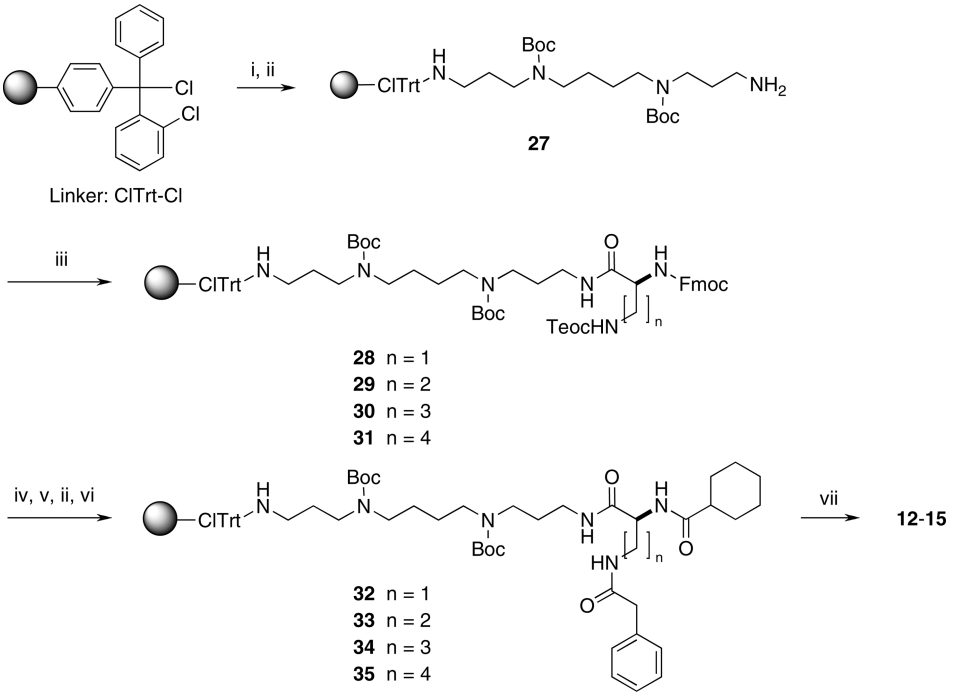

[a] Reagents: (i) $H_2N(CH_2)_3NBoc(CH_2)_4NBoc(CH_2)_3NHTeoc$ (1.1 equiv), *i*Pr_2EtN (5 equiv), CH_2Cl_2, 2 days; (ii) Bu_4NF (4 equiv), DMF, 50 °C, 1 h, then room temperature, 2 h; (iii) Fmoc-aa(Teoc)-OH **18**−**21** (3 equiv), DIC (3 equiv), HOBt (3 equiv), DMF, 24 h; (iv) 20% piperidine−DMF, 2 × 10 min; (v) cyclohexanecarboxylic acid (3 equiv), DIC (3 equiv), HOBt (3 equiv), DMF, 16 h; (vi) $PhCH_2COOPfp$ (3 equiv), *i*Pr_2EtN (3 equiv), DMF, 16 h; (vii) 20% TFA−CH_2Cl_2 (30 min and then 2 × 15 min).

inhibition at 0.1 μM (35−77%) was roughly similar to that caused by **2** (59%). Thus, even rather drastic structural modifications of the headgroup of PhTX-343 appear to have a limited effect on the inhibitory activity at the $GluA1_i$ AMPA receptor. By contrast, several of the analogues showed increased inhibition of the GluN1/2A NMDA receptor as compared to **2** (Figure 2). The latter compound gave 9% and 61% inhibition at the concentrations 0.1 and 10 μM, respectively, whereas especially **10** and **13** displayed improved activity with 63% and 36% inhibition at 0.1 μM and 92% and 94% inhibition at 10 μM, respectively. No improvement in potency on either of the two targets was observed upon extension of the polyamine chain of **2** with β-alanine (compound **3**) or ω-guanidinylated α,ω-diamino acids (compounds **4** and **5**).

Furthermore, IC_{50} values for the inhibition by **6**−**11** at the $GluA1_i$ AMPA receptor and by **6**−**15** at the GluN1/2A NMDA receptor were determined (Tables 1 and 2; examples of concentration−inhibition curves are shown in Figure 3). In general, the toxins containing the *N*-acylated cyclohexylalanine moiety (**6**−**11**), instead of the *N*-butyryltyrosine moiety present in **2**, were significantly more potent at the $GluA1_i$ AMPA receptor (IC_{50} values in the range 10−100 nM) as compared to the GluN1/2A NMDA receptor (IC_{50} values 0.6−4.4 μM) (Table 1). However, some notable exceptions were observed. Thus, the very potent *N*-(1-naphthyl)acetyl analogue **10** was equipotent at both receptors (IC_{50} values 41 and 47 nM, respectively) and the ratios between the IC_{50} values for the two receptors were only 17 and 8 for **9** and **11**, respectively (Table 1). These analogues have the most bulky

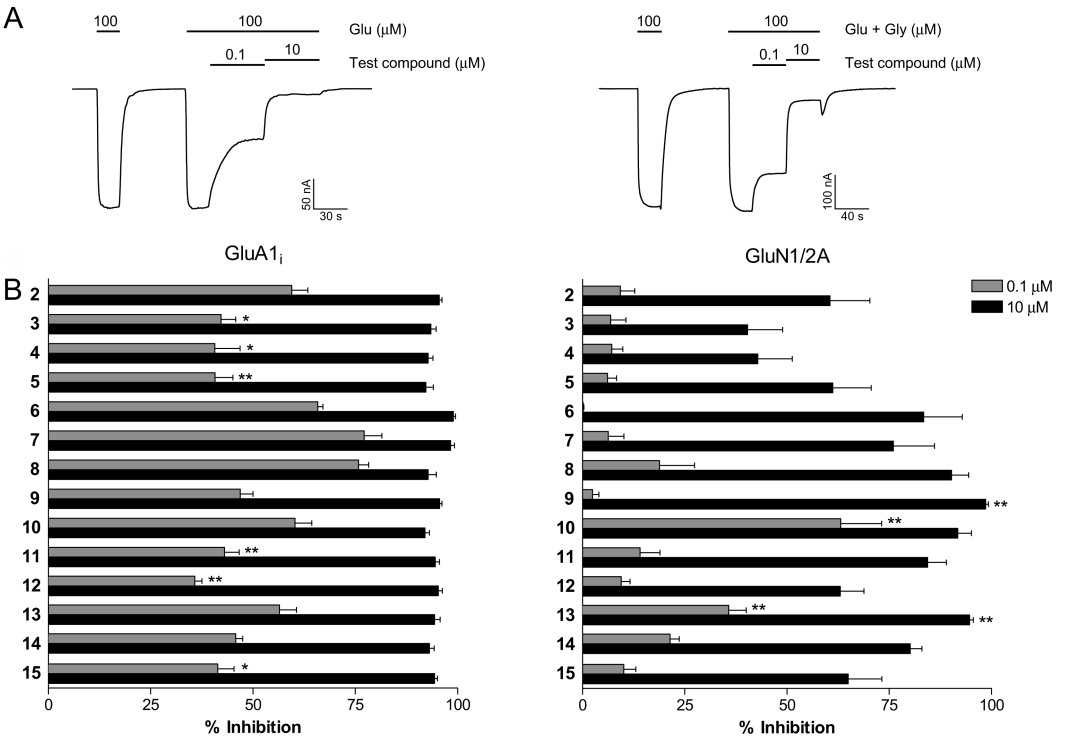

Figure 2. Inhibitory activities of toxin analogues expressed as their ability to decrease transmembrane currents elicited by glutamate in oocytes expressing either the homomeric $GluA1_i$ AMPA receptors or the heteromeric GluN1/2A NMDA receptors. Toxins were coapplied with glutamate (100 μM) or glutamate and glycine (100 μM each) at concentrations of 0.1 or 10 μM. (A) Two-electrode voltage clamp (−60 mV) recordings of currents from an oocyte expressing the $GluA1_i$ receptors (left) and GluN1/2A receptors (right). (B) Inhibitions achieved with 0.1 and 10 μM concentrations of the toxins. Bars show mean % inhibition ± SEM ($n \geq 3$). The significance of differences between the values for individual analogues and that for **2** are indicated as follows: *, $p < 0.05$; **, $p < 0.01$.

Table 1. Antagonist Effect of Cyclohexylalanine-Containing Analogues **6**−**11** on $GluA1_i$ AMPA and GluN1/2A NMDA Receptors

	IC_{50}[a]		
compd	$GluA1_i$	GluN1/2A	selectivity[b]
2	23 nM ± 4% (8)	2739 nM ± 14% (3)	119
6	32 nM ± 16% (3)	4383 nM ± 10% (3)	137
7	11 nM ± 19% (3)	2567 nM ± 14% (3)	233
8	21 nM ± 5% (3)	656 nM ± 13% (3)	31
9	87 nM ± 10% (3)	1446 nM ± 9% (4)	17
10	41 nM ± 10% (4)	47 nM ± 17% (7)	1
11	105 nM ± 13% (6)	794 nM ± 11% (4)	8

[a] Calculated from the decrease of current, elicited by either 100 μM glutamate ($GluA1_i$ AMPA receptor) or 100 μM glutamate and 100 μM glycine (GluN1/2A NMDA receptor), by simultaneous coapplication of the antagonist on oocytes expressing the respective receptor. All measurements were conducted at the holding potential −60 mV. The IC_{50} values are given as mean ± % difference between IC_{50} and antilog to ($\log IC_{50}$ + SEM). Number of replicates is indicated in parentheses. [b] Ratio between IC_{50} (GluN1/2A) and $IC_{50}(GluA1_i)$.

Table 2. Antagonist Effect of Compounds **12**−**15** on the GluN1/2A NMDA Receptor

compd	IC_{50}[a]
2	2739 nM ± 14% (3)
12	2805 nM ± 13% (6)
13	106 nM ± 14% (5)
14	1026 nM ± 10% (6)
15	1349 nM ± 24% (4)

[a] Calculated from decrease of current elicited by 100 μM glutamate by simultaneous coapplication of the antagonist on oocytes expressing the heteromeric GluN1/2A NMDA receptor. All measurements were conducted at the holding potential −60 mV. IC_{50} values are given as mean ± % difference between IC_{50} and antilog to ($\log IC_{50}$ + SEM). Number of replicates is indicated in parentheses.

apolar *N*-acyl groups. For compound **10**, a conspicuous 58-fold improvement in the potency relative to **2** was achieved on the GluN1/2A NMDA receptor. In the case of the $GluA1_i$ AMPA receptor, only compound **7**, containing an *N*-cyclopropylcarbonyl group, displayed slightly higher potency than the parent compound **2** (IC_{50} values of 11 and 23 nM, respectively). For this analogue, the selectivity index between $GluA1_i$ AMPA and GluN1/2A NMDA receptors reached the highest value of 233.

The novel diamino acid-based analogues **12**−**15**, with systematically varied length of the spacer separating the apolar cyclohexyl and benzyl groups present in these derivatives, were approximately equipotent with **2** on the $GluA1_i$ AMPA receptor (Figure 2) but exhibited increased potency on the GluN1/2A NMDA receptor (Table 2). At the same time, information about the importance of the relative positions of the cyclohexyl group and the benzyl group was provided. Thus, the maximum inhibitory activity was achieved with compound **13** (two methylene and one methine group separating the nitrogen atoms of the diamino acid moiety, Figure 1), for which the IC_{50} value was 106 nM. Compound **12** was equipotent with **2**, while compounds **14** and **15** were roughly twice as potent. The potency of **13** on the GluN1/2A NMDA receptor was improved 26-fold relative to **2**.

Finally, holding potential dependency of the inhibition was determined for **2** and **6**−**11** at −40, −60, and −80 mV (Figure 3). The inhibitory activity was measured at the concentrations corresponding to the IC_{50} value determined at the holding potential −60 mV (Table 1). Generally, the toxins exhibited considerably decreased inhibition as the holding potential became less negative. Inhibition of the $GluA1_i$ AMPA receptor was somewhat less voltage-dependent as compared to the GluN1/2A NMDA receptor under the conditions used. Thus,

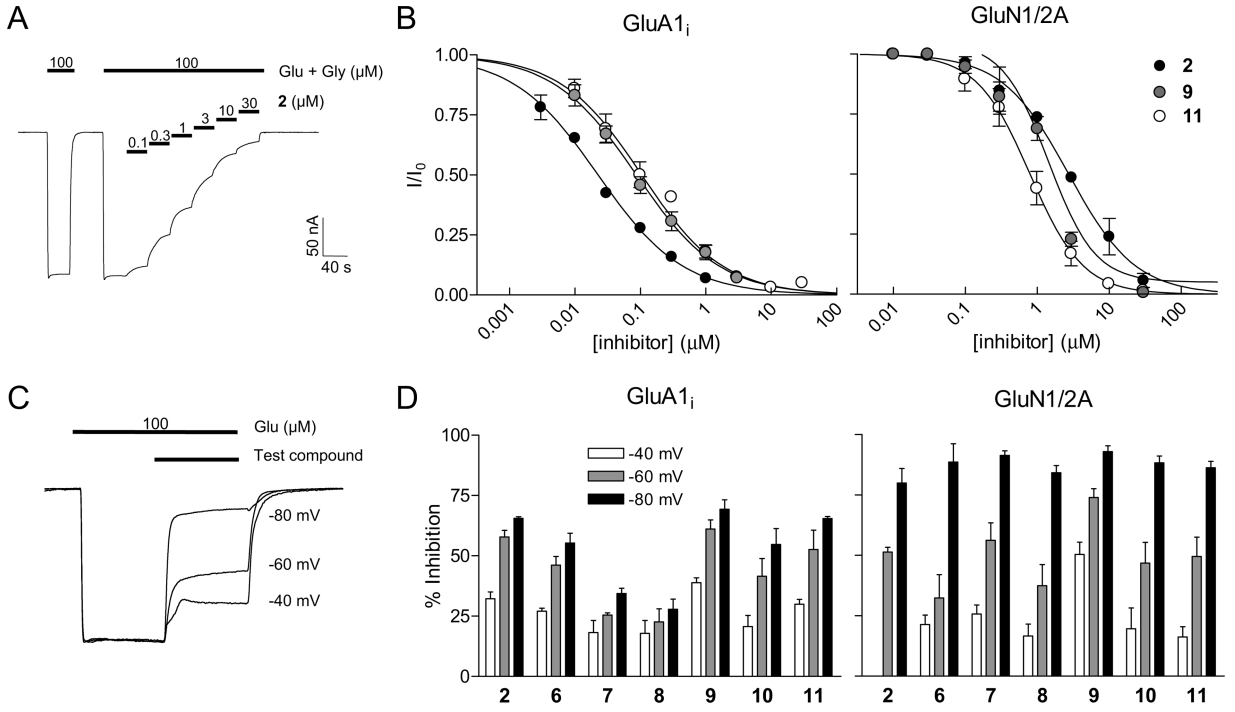

Figure 3. Inhibition of response to glutamate by toxin analogues in oocytes expressing the homomeric $GluA1_i$ AMPA receptors or the heteromeric GluN1/2A NMDA receptors. (A) Receptor currents in response to coapplication of glutamate and glycine (100 μM each) with increasing concentrations of **2** for the GluN1/2A NMDA receptor at holding potential −60 mV. (B) Concentration−inhibition curves for antagonism of response to glutamate (100 μM) or glutamate and glycine (100 μM each) by **2**, **9**, and **11** at holding potential −60 mV; the data points represent normalized receptor currents ± SEM (n = 3). (C) Receptor current measured in response to coapplication of glutamate (100 μM) with test compound for the $GluA1_i$ receptor at holding potential −40, −60, and −80 mV. (D) Holding potential dependency of the inhibition by toxin analogues **6**−**11** for holding potentials −40, −60, and −80 mV at toxin concentrations equal to their IC_{50} values determined at −60 mV (Table 1).

at the concentrations studied, all analogues except **10** retained at least half of the potency exhibited at the $GluA1_i$ AMPA receptor at −80 mV when the potential was changed to −40 mV. In the case of **10**, the compound with the most pronounced voltage dependence, only 38% of the potency exhibited at −80 mV was retained at −40 mV, whereas the least voltage-dependent inhibitor was compound **8**. At the GluN1/2A NMDA receptor, on the other hand, the analogues retained only about one-fourth of the potency shown at −80 mV when tested at the holding potential of −40 mV, the only exception being compound **9**, which proved to be the least voltage-dependent inhibitor of the GluN1/2A NMDA receptor (Figure 3). The observed trends in voltage dependency are similar to those previously reported for memantine at different NMDA receptor subunit combinations.[39,40] However, in contrast to memantine, which has a rather weak NMDA receptor affinity, compound **10** is one of the most potent NMDA receptor blockers identified so far[41,42] and may prove to be a useful tool for studies of NMDA receptors.

This work furthermore demonstrates that the activity of the philanthotoxin analogues on the iGluR subtypes studied in the present investigation was governed by fine structural requirements in the case of the GluN1/2A NMDA receptor, whereas the activity at the $GluA1_i$ AMPA receptor only varied by less than 1 order of magnitude across the panel of the analogues studied. This indicates that the affinity for the latter receptor is mediated mainly by the polyamine moiety and is affected to a lesser extent by the structure of the headgroup. By contrast, a span of 2 orders of magnitude in potency was observed for the GluN1/2A NMDA receptor, with the most potent analogues having an aromatic substituent in the headgroup. Especially interesting is the finding of a pronounced dependence of activity on the GluN1/2A NMDA receptor on the structure of the diamino acid, indicating the presence of well-defined interaction sites.

Conclusion

In the present work, use of various solid-phase synthetic approaches resulted in the preparation of an array of PhTX-343 (**2**) analogues with structurally diverse head groups. The analogues were evaluated for their ability to antagonize glutamate-elicited currents on $GluA1_i$ AMPA and GluN1/2A NMDA receptors. The antagonism at the $GluA1_i$ AMPA receptor was largely insensitive to the structure of the headgroup, as all investigated analogues exhibited similar potency compared to that of the parent compound **2**. These observations are in agreement with our earlier studies on structure−activity relationships for philanthotoxin analogues using kainate-induced currents in rat brain AMPA receptors expressed in *Xenopus laevis* oocytes.[27]

By contrast, investigation of the inhibition of the GluN1/2A NMDA receptor revealed that the presence of a cyclohexyl group together with a bulky acyl group gives rise to a significant increase of the potency. While compounds **6** and **7**, containing small acyl substituents, exhibited potencies similar to or lower than that of **2**, compounds **8**−**11**, with a bulky aliphatic or aromatic acyl group, exhibited significantly improved potencies. For compound **10**, the determined IC_{50} value reached 47 nM. Our results also provide directions for future studies of synthetic analogues bearing aromatic substituents along with a cyclohexyl group, possibly interacting with the receptor by π and hydrophobic interactions, respectively.

The results for compounds **12**−**15** demonstrate the need for a proper distance between the aromatic and the alicyclic group. Thus, the discovery of the nanomolar antagonist **13** could provide a novel design strategy to even more potent analogues based on diamino acids replacing the traditional, α-amino acid-based strategies exploited in previous investigations of structure−activity relationships for philanthotoxin analogues.

Experimental Section

Chemistry. General Procedures. Unless otherwise stated, starting materials and solvents were purchased from commercial suppliers (IRIS Biotech, Aldrich, or Fluka) and used as received. CH_2Cl_2 was distilled from P_2O_5 and stored over 4 Å molecular sieves. ^{1}H NMR and ^{13}C NMR spectra were recorded at 300.06 and 75.45 MHz, respectively, on a Varian Mercury Plus or a Gemini 2000 spectrometer, using $CDCl_3$ or CD_3OD as solvents and tetramethylsilane (TMS) as internal standard. Coupling constants (*J* values) are given in hertz (Hz), and multiplicities of ^{1}H NMR signals are reported as follows: s, singlet; d, doublet; t, triplet; q, quartet; p, pentet; sx, sextet; m, mulitplet; br, broad. High-resolution mass spectrometric (HRMS) measurements were performed on a Bruker APEX Qe Fourier transform mass spectrometer equipped with a 9.4 T superconducting cryomagnet and an external electrospray ion source (Apollo II source). The spectra were externally calibrated with arginine cluster in positive mode. The samples were dissolved in MeOH and introduced into the electrospray ion source using a syringe pump with a flow of 2 μL/min. Solid-phase reactions were performed in Teflon filter vessels on a Scansys PLS 4 × 6 organic synthesizer equipped with a heating block. The preparative Agilent 1100 HPLC system consisted of 2 preparative pump units, a UV detector, and a Phenomenex Luna C18(2) (5 μm) column (22.1 mm × 250 mm). Eluents were composed by mixing solvent A (MeCN−H_2O−TFA 5:95:0.1) and B (MeCN−H_2O−TFA 95:5:0.1) at a flow rate of 20 mL/min (elution gradient profiles are given below for each compound subtype). TLC separations were performed using Merck silica gel 60 F_{254} (0.2 mm) precoated plates. Vacuum liquid chromatography (VLC) was performed using Merck silica gel 60H (particle size: 90% < 55 μm).

Analytical HPLC was performed on a Shimadzu system consisting of an SCL-10A VP controller, an SIL-10AD VP autosampler, an LC-10AT VP pump, an SPD-M10A VP diode array detector, and a CTO-10AC VP column oven, using a Phenomenex Luna C18(2) (3 μm) column (4.6 mm × 150 mm). The HPLC system was controlled by Class VP 6 software. Eluents were composed by mixing solvent C (MeCN−H_2O−HCOOH 5:95:0.1) and solvent D (MeCN−H_2O−HCOOH 95:5:0.1) at a flow rate of 0.8 mL/min; a linear gradient rising from 0% D to 100% D during 30 min was employed for compounds **4**, **5**, and **7**−**15**, whereas a two-step gradient rising linearly from 0% D to 80% D during 5 min and then to 100% D during 25 min was employed for protected amino acid building blocks **16**−**21**.

Purities of all tested compounds were determined by the above HPLC methods and were in each case measured to be higher than 95% by UV detection; specific retention times and purities are given for the individual compounds.

Fmoc-hArg(Boc$_2$)-OH (16). To a solution of Fmoc-Lys(Boc)-OH (1.50 g, 3.21 mmol) in CH_2Cl_2 (25 mL) was added TFA (25 mL). The mixture was stirred for 1 h at room temperature and then concentrated in vacuo. The residue was coevaporated with toluene (3 × 10 mL) to remove TFA. The residue was dissolved in DMF (15 mL), *i*Pr_2EtN (2.8 mL, 5 × 3.21 mmol), and then pyrazol(Boc)$_2$ (1.19 g, 1.2 × 3.21 mmol) in DMF (2 mL) were added, and the mixture was stirred for 16 h. Ice (50 mL) was added to the reaction mixture, resulting in formation of a precipitate. The mixture was acidified with 1 M HCl to pH 5 and extracted with EtOAc (100 mL); the organic layer was washed with H_2O (5 × 100 mL) and brine (100 mL), dried (Na_2SO_4), and concentrated in vacuo. The residue was dissolved in CH_2Cl_2 and loaded onto a VLC column (5 cm × 6 cm), which was eluted with hexane, hexane−EtOAc (10:1) and then with hexane−EtOAc−HOAc (80:20:0.1 to 100:50:0.15). The appropriate fractions (R_f 0.2 with hexane−EtOAc−HOAc 100:50:0.75) were evaporated and treated as in general procedure A to give the product **16** (1.61 g, 81%); t_R = 17.44 min (96.8% at 220 nm); $[\alpha]_D^{23}$ = +16.6 (*c* 1.0, $CHCl_3$). HRMS: calcd for $C_{32}H_{43}N_4O_8$ $[M + H]^+$ 611.30754, found 611.30734. ^{1}H NMR (300 MHz, $CDCl_3$): δ 7.75 (2H, br d, *J* = 7.3 Hz, Fmoc ArH), 7.61 (2H, m, Fmoc ArH), 7.39 (2H, br t, *J* = 7.3 Hz, Fmoc ArH), 7.30 (2H, br t, *J* = 7.3 Hz, Fmoc ArH), 4.40 (1H, br m, H-α), 4.37 (2H, d, *J* = 7.0 Hz, Fmoc-CH_2), 4.21 (1H, t, *J* = 7.0 Hz, Fmoc-CH), 3.50 (2H, br m, H-ε), 1.94 (1H, br m, H_A-β), 1.82 (1H, br m, H_B-β), 1.64 (2H, br m, H-δ), 1.56−1.24 (2H, br m, H-γ), 1.50 (9H, s, C[CH_3]$_3$), 1.49 (9H, s, C[CH_3]$_3$). ^{13}C NMR (75 MHz, $CDCl_3$): δ 174.7, 161.2, 156.1, 155.7, 153.0, 143.9, 143.7, 141.3 (2C), 127.7, 127.1, 125.2 (2C), 120.0 (2C), 84.1, 81.2, 67.2, 53.7, 47.3, 41.4, 31.9, 28.6, 28.3 (3C), 28.2 (3C), 22.4.

Boc-gDap(Boc$_2$)-OH (17). Boc-Dap-OH (0.80 g, 3.92 mmol) was dissolved in DMF (10 mL); *i*Pr_2EtN (1.36 mL, 2 × 3.92 mmol) and pyrazol(Boc)$_2$ (1.46 g, 1.2 × 3.92 mmol) in DMF (5 mL) were added, and the mixture was stirred for 16 h at room temperature. Ice (50 mL) was added to the reaction mixture, resulting in formation of a precipitate. The mixture was acidified with 1 M HCl to pH 5 and extracted with EtOAc (200 mL); the organic layer was washed with H_2O (5 × 100 mL) and brine (100 mL), dried (Na_2SO_4), and concentrated in vacuo. The residue was dissolved in CH_2Cl_2 and loaded onto a VLC column (5 cm × 6 cm), which was eluted with hexane, hexane−EtOAc (10:1), and then hexane−EtOAc−HOAc (80:20:0.1 to 100:50:0.15). The appropriate fractions (R_f 0.2 with hexane−EtOAc−HOAc 100:50:0.75) were evaporated to give **17** (1.51 g, 87%); t_R = 14.99 min (99.3% at 220 nm); $[\alpha]_D^{23}$ = +6.8 (*c* 1.1, $CHCl_3$). HRMS: calcd for $C_{19}H_{34}N_4O_8$ $[M + H]^+$ 447.24494, found 447.24498. ^{1}H NMR (300 MHz, $CDCl_3$): δ 4.30 (1H, br m, H-α), 4.02 (1H, br d, *J* = 14.7 Hz, H_A-β), 3.44 (1H, dd, *J* = 14.7 and 4.1 Hz, H_B-β), 1.50 (9H, s, C[CH_3]$_3$), 1.49 (9H, s, C[CH_3]$_3$), 1.44 (9H, s, C[CH_3]$_3$). ^{13}C NMR (75 MHz, $CDCl_3$): δ 171.5, 159.9, 156.4, 156.0, 152.3, 84.8, 82.0, 80.4, 56.2, 46.1, 28.5 (3C), 28.2 (6C).

Teoc Side-Chain Protection in Diamino Acids. General Procedure A. To Na_2CO_3 (1 equiv) in H_2O (3 mL/mmol) was added Fmoc-aa-OH (1 equiv) in dioxane−H_2O (1:1, 8 mL/mmol), followed by Teoc-ONp (1.1 equiv) in dioxane (4 mL/mmol). The mixture was stirred for 16 h. The clear reaction mixture was neutralized with 1 M HCl (3−4 mL/mmol) and was then diluted with EtOAc (~50 mL/mmol) and 1 M HCl (5 mL/mmol). The phases were separated; the aqueous phase was extracted with EtOAc (25 mL/mmol), and the combined organic layers were washed with H_2O (3 × 35 mL/mmol) and brine (35 mL/mmol), dried (Na_2SO_4), and concentrated in vacuo. The residue was dissolved in CH_2Cl_2 and loaded onto a VLC column (6 cm × 7 cm, 1.5−3.5 mmol scale), which was eluted with hexane, hexane−EtOAc (10:1) and then with hexane−EtOAc−HOAc (100:20:0.12 to 50:50:0.1). The appropriate fractions (R_f 0.2 with hexane−EtOAc−HOAc 100:50:0.75) were evaporated, and the resulting syrup was coevaporated with toluene−CH_2Cl_2 1:1 (3×) to remove HOAc. Upon drying for 16 h the product was obtained as a white solid.

Fmoc-Dap(Teoc)-OH (18). Preparation from Fmoc-Dap-OH (3.5 mmol) using general procedure A gave **18** (1.65 g, 81%); t_R = 15.46 min (99.5% at 254 nm); $[\alpha]_D^{23}$ = +5.1 (*c* 1.1, $CHCl_3$). HRMS: calcd for $C_{24}H_{30}N_2O_6SiNa$ $[M + Na]^+$ 493.17653, found 493.17649. ^{1}H NMR (300 MHz, $CDCl_3$): δ 7.76 (2H, d, *J* = 7.3 Hz, Fmoc ArH), 7.63−7.55 (2H, br m, Fmoc ArH), 7.40 (2H, t, *J* = 7.3 Hz, Fmoc ArH), 7.31 (2H, t, *J* = 7.3 Hz, Fmoc ArH), 4.50−4.10 (5H, br m, H-α, Fmoc-CH_2 and −C*H*, and Teoc O-CH_2), 3.78−3.53 (2H, br m, H-β), 0.98 (2H, br m, Teoc Si-CH_2), 0.00 (9H, br s, Teoc Si[CH_3]$_3$). ^{13}C NMR (75 MHz, $CDCl_3$): δ 173.3, 172.9*, 158.9*, 158.0†, 156.6†, 155.8*†, 143.7, 143.6, 141.3 (2C), 127.8 (2C), 127.1 (2C), 125.2 (2C), 120.0

(2C), 67.6, 65.0*, 64.1†, 55.1, 54.3*, 47.2, 43.0*, 42.5, 17.8, −1.3 (* designates signals due to the presence of two rotamers, † designates broadened signals).

Fmoc-Dab(Teoc)-OH (19). Preparation from Fmoc-Dab-OH (1.5 mmol) using general procedure A gave **19** (0.73 g, 84%); t_R = 15.34 min (99.7% at 254 nm); $[\alpha]_D^{23}$ = +3.7 (*c* 1.1, $CHCl_3$). HRMS: calcd for $C_{25}H_{32}N_2O_6SiNa$ $[M + Na]^+$ 507.19218, found 507.19206. ^{1}H NMR (300 MHz, $CDCl_3$): δ 7.77 (2H, d, *J* = 7.3 Hz, Fmoc ArH), 7.64−7.58 (2H, br m, Fmoc ArH), 7.41 (2H, t, *J* = 7.3 Hz, Fmoc ArH), 7.32 (2H, t, *J* = 7.3 Hz, Fmoc ArH), 4.50−4.10 (6H, br m, Fmoc-C*H*$_2$ and −C*H*, Teoc O-C*H*$_2$, and H-α), 3.55−3.00 (2H, br m, H-*γ*), 2.14−1.85 (2H, br m, H-*β*), 1.02 (2H, br m, Teoc Si-C*H*$_2$), 0.04 (9H, br s, Teoc Si[C*H*$_3$]$_3$). ^{13}C NMR (75 MHz, $CDCl_3$): δ 175.2†, 158.6*, 157.6†, 156.4†, 143.8, 143.6, 141.3 (2C), 127.7 (2C), 127.1 (2C), 125.1 (2C), 120.0 (2C), 67.3, 64.6*, 63.8†, 51.5, 47.3, 37.0, 33.4, 32.1*, 17.9, −1.2 (* designates signals due to the presence of two rotamers, † designates broadened signals).

Teoc Side-Chain Protection in Diamino Acids. General Procedure B. To a solution of Fmoc-aa(Boc)-OH (2.54 mmol) in CH_2Cl_2 (20 mL) was added TFA (20 mL). The mixture was stirred for 2 h at room temperature, concentrated in vacuo, and coconcentrated with toluene (3 × 10 mL) to remove TFA. The residue was dissolved in DMF (10 mL) and *i*Pr$_2$EtN (8.36 mmol, 1.44 mL) was added, followed by Teoc-ONp (4.77 mmol, 1.88 equiv) in DMF (2 mL). After stirring for 16 h at room temperature, the mixture was diluted with EtOAc (100 mL) and 0.1 M HCl (75 mL). The phases were separated; the aqueous phase was extracted with EtOAc (100 mL), the combined organic layers were washed with H_2O (5 × 100 mL) and brine (2 × 100 mL), dried (Na_2SO_4), and concentrated in vacuo. The residue was dissolved in CH_2Cl_2 and loaded onto a VLC column (5 cm × 6 cm), which was eluted with hexane, hexane−EtOAc (10:1), and hexane−EtOAc−HOAc (80:20:0.1 to 100:50:0.15). The product was isolated as in general procedure A.

Fmoc-Orn(Teoc)-OH (20). Preparation from Fmoc-Orn(Boc)-OH using general procedure B gave **20** (1.02 g, 80%); t_R = 15.35 min (99.9% at 254 nm); $[\alpha]_D^{23}$ = +10.8 (*c* 1.1, $CHCl_3$). HRMS: calcd for $C_{26}H_{34}N_2O_6SiNa$ $[M + Na]^+$ 521.20783, found 521.20772. ^{1}H NMR (300 MHz, $CDCl_3$): δ 7.75 (2H, d, *J* = 7.3 Hz, Fmoc ArH), 7.63−7.50 (2H, br m, Fmoc ArH), 7.38 (2H, t, *J* = 7.3 Hz, Fmoc ArH), 7.29 (2H, t, *J* = 7.3 Hz, Fmoc ArH), 4.53−4.03 (6H, br m, Fmoc-C*H*$_2$ and −C*H*, Teoc O-C*H*$_2$, and H-α), 3.25−3.05 (2H, br m, H-*δ*), 2.02−1.36 (4H, br m, H-*β* and H-*γ*), 0.98 (2H, br m, Teoc O-C*H*$_2$), 0.04 (9H, br s, Teoc Si[C*H*$_3$]$_3$). ^{13}C NMR (75 MHz, $CDCl_3$): δ 175.5, 175.2*, 156.7†, 156.2†, 143.8, 143.6, 141.3 (2C), 127.7 (2C), 127.1 (2C), 125.2 (2C), 120.0 (2C), 67.6*, 67.2, 63.6†, 54.1*, 53.5, 47.3, 40.5†, 29.7, 26.0†, 17.9, −1.2 (* designates signals due to the presence of two rotamers, † designates broadened signals).

Fmoc-Lys(Teoc)-OH (21). Preparation from Fmoc-Lys(Boc)-OH using general procedure B gave **21** (0.75 g, 58%); t_R = 15.67 min (99.8% at 254 nm); $[\alpha]_D^{23}$ = +15.6 (*c* 1.1, $CHCl_3$). ^{1}H NMR (300 MHz, $CDCl_3$): δ 7.75 (2H, d, *J* = 7.3 Hz, Fmoc ArH), 7.63−7.51 (2H, br m, Fmoc ArH), 7.38 (2H, t, *J* = 7.3 Hz, Fmoc ArH), 7.29 (2H, t, *J* = 7.3 Hz, Fmoc ArH), 4.55−4.00 (6H, br m, Fmoc-C*H*$_2$ and −C*H*, and Teoc O-C*H*$_2$, and H-α), 3.27−3.00 (2H, br m, H-*ε*), 2.00−1.25 (6H, br m, H-*β*, H-*γ*, and H-*δ*), 0.98 (2H, br m, Teoc O-C*H*$_2$), 0.02 (9H, br s, Teoc Si[C*H*$_3$]$_3$). ^{13}C NMR (75 MHz, $CDCl_3$): δ 175.7, 175.5*, 156.1†, 143.9, 143.7, 141.3 (2C), 127.7 (2C), 127.0 (2C), 125.1 (2C), 119.9 (2C), 67.7*, 67.1, 63.7†, 54.4*, 53.7, 47.3, 40.7†, 31.9†, 29.4†, 22.2†, 17.9, −1.2 (* designates signals due to the presence of two rotamers, † designates broadened signals).

SPS of Philanthotoxin Analogues Elongated with an Amino Acid. General Procedure C. To batches of BAL resin (100 mg, 0.9 mmol/g) in Teflon filter vessels was added a mixture of $NaBH(OAc)_3$ (10 equiv) and $H_2N(CH_2)_3NBoc(CH_2)_4NBoc(CH_2)_3NHTeoc$[25] (10 equiv) in HOAc−DMF (1:9, 5 mL). The resin was agitated for 16 h, followed by draining and washing with DMF, MeOH, DMF, and CH_2Cl_2 (each 3 × 5 mL for 5 min). Fmoc-Tyr(*t*Bu)-OH (4 equiv), preactivated for 10 min with TFFH (4 equiv) and *i*Pr$_2$EtN (8 equiv) in DMF (5 mL), was added, and the resin was agitated for 3 h and then washed with DMF (3×), after which the coupling was repeated for 16 h. The resin was washed with DMF and CH_2Cl_2 (3×), Fmoc-deprotected with 20% piperidine−DMF (3 mL, 2 × 10 min) followed by washing with DMF (5×). The resin was suspended in dry DMF (1 mL), and $C_3H_7COOPfp$ (5 equiv) and *i*Pr$_2$EtN (5 equiv) in dry DMF (2 mL) were added. The resin was agitated at room temperature under N_2 for 16 h, after which the resulting resin **22** was filtered and washed with DMF, MeOH, and CH_2Cl_2 (3×). Teoc-removal with Bu_4NF (3 equiv) in dry DMF (3 mL) at 50 °C for 1 h, followed by washing with DMF (3×), was performed twice. The resin was then washed with MeOH, DMF, and CH_2Cl_2 (3×). The resin batches were treated with **16** or **17** (3 equiv), DIC (3 equiv), and HOBt (3 equiv) in dry DMF (5 mL), and the mixture was agitated for 3 h. After washing with DMF (3×), the coupling was repeated for 16 h. The resin was washed with DMF, MeOH, DMF, and CH_2Cl_2 (3×). In the case of coupling with **16**, the resin was treated with 20% piperidine−DMF (3 mL, 2 × 10 min). Cleavage was performed with 50% TFA−CH_2Cl_2 (3 mL) for 1 h. The filtrate was collected by draining, and the resin was washed with MeOH and CH_2Cl_2 (each 2 × 5 mL). The combined filtrates were concentrated and then coevaporated with toluene and MeOH (each 3 × 5 mL), and the residue was dried overnight. Purification of the crude by preparative HPLC (using a linear gradient rising from 5% of B to 20% of B during 20 min) afforded **4** and **5** as the tetrakis(TFA) salts.

Compound 4. Yield: 33 mg (36%); t_R = 10.72 min (99.1% at 220 nm). HRMS: calcd for $C_{27}H_{49}N_9O_4$ $[M + H]^+$ 564.39803, found 564.39804. ^{1}H NMR (300 MHz, CD_3OD): δ 7.06 (2H, d, *J* = 8.5 Hz, H-b/H-b′), 6.71 (2H, d, *J* = 8.5 Hz, H-c/H-c′), 4.38 (1H, t, *J* = 7.8 Hz, H-α), 4.13 (1H, br t, *J* = 6.8 Hz, H-α′), 3.76 (1H, dd, *J* = 15.0 and 5.6 Hz, H$_A$-*β*′), 3.64 (1H, dd, *J* = 15.0 and 7.6 Hz, H$_B$-*β*′), 3.48−3.12 (4H, br m, 2× −CH$_2$-NH), 3.07 (4H, m, 2× −CH$_2$-NH), 3.01−2.92 (3H, br m, H$_A$-*β* and −CH$_2$-NH), 2.89−2.80 (3H, br m, H$_B$-*β* and −CH$_2$-NH), 2.18 (2H, t, *J* = 7.3 Hz, H-2′), 1.94 (2H, m, −CH$_2$−), 1.79 (6H, m, 3× −CH$_2$−), 1.56 (2H, sx, *J* = 7.3 Hz, H-3′), 0.87 (3H, t, *J* = 7.3 Hz, H-4′). ^{13}C NMR (75 MHz, CD_3OD): δ 176.0, 174.9, 168.1, 159.0, 157.2, 131.1 (2C), 128.7 (2C), 116.2, 57.1, 53.4, 48.2, 46.5, 46.2, 43.0, 38.6, 37.9, 37.6, 36.7, 27.4, 27.3, 24.3 (2C), 20.3, 14.0.

Compound 5. Yield: 44 mg (46%); t_R = 10.84 min (>99.9% at 220 nm). HRMS: calcd for $C_{30}H_{55}N_9O_4$ $[M + H]^+$ 606.44498, found 606.44517. ^{1}H NMR (300 MHz, CD_3OD): δ 7.06 (2H, d, *J* = 8.5 Hz, H-b/H-b′), 6.71 (2H, d, *J* = 8.5 Hz, H-c/H-c′), 4.38 (1H, t, *J* = 7.8 Hz, H-α), 3.86 (1H, t, *J* = 6.6 Hz, H-α′), 3.48−3.17 (6H, br m, 2× −CH$_2$-NH and H-*ε*′), 3.06 (4H, m, 2 × −CH$_2$-NH), 3.01−2.93 (3H, br m, H$_A$-*β* and −CH$_2$-NH), 2.89−2.80 (3H, br m, H$_B$-*β* and −CH$_2$-NH), 2.18 (2H, t, *J* = 7.3 Hz, H-2′), 1.94 (2H, m, −CH$_2$−), 1.87 (2H, m, H-*β*′), 1.79 (6H, m, 3× −CH$_2$−), 1.63 (2H, m, H-*δ*′), 1.56 (2H, sx, *J* = 7.3 Hz, H-3′), 1.47 (2H, m, H-*γ*′), 0.86 (3H, t, *J* = 7.3 Hz, H-4′). ^{13}C NMR (75 MHz,, CD_3OD): δ 176.0, 174.9, 170.7, 158.5, 157.2, 131.1 (2C), 128.7 (2C), 116.2, 57.0, 54.3, 48.2, 46.5, 46.2, 42.0, 38.6, 37.9, 37.4, 36.8, 32.2, 29.4, 27.4 (2C), 24.3 (2C), 23.2, 20.3, 14.0.

SPS of Cyclohexylalanine-Containing Philanthotoxin Analogues. General Procedure D. In a syringe (20 mL, fitted with a polypropylene filter and a Teflon valve), trityl chloride resin (1.66 g, 2.2 mmol/g) was swelled in dry CH_2Cl_2. After draining, the resin was treated with 10% *i*Pr$_2$EtN−CH_2Cl_2 for 5 min, and then washed with CH_2Cl_2 (2 × 5 min). A solution of $H_2N(CH_2)_3$-$NBoc(CH_2)_4NBoc(CH_2)_3NHTeoc$[25] (2.00 g, 1 × 3.65 mmol) and *i*Pr$_2$EtN (1.9 mL, 3 × 3.65 mmol) in CH_2Cl_2 (25 mL) was added to the resin in a round-bottom flask (50 mL), and the suspension was stirred gently for 3 days. The resin was transferred to the syringe, washed with CH_2Cl_2 (2 × 15 mL, each 5 min), and capping of unreacted linker groups was performed with *i*Pr$_2$EtN−MeOH−CH_2Cl_2 (5:15:80, 2 × 15 mL, each 15 min). The resin was drained

and washed with CH_2Cl_2, DMF, and CH_2Cl_2 (each 3×), transferred to a round-bottom flask (100 mL), and Teoc-deprotection was performed with Bu_4NF (3 equiv) in dry DMF (50 mL) at 50 °C for 1 h and then at room temperature for 1 h. The resin was transferred to the syringe, drained, and washed with DMF, MeOH, DMF, and CH_2Cl_2 (each 3×) and finally dried overnight to yield resin **25** (2.93 g, ∼1.2 mmol/g). The resin was preswollen in dry DMF (5 mL). A mixture of Fmoc-Cha-OH (3 equiv), DIC (3 equiv), and HOBt (3 equiv) in dry DMF (30 mL) was stirred for 20 min, filtered, and added to the resin, and the mixture was stirred gently for 20 h. The resin was transferred to the syringe and washed with DMF, MeOH, DMF, and CH_2Cl_2 (each 3×). After drying, portions of the resin (0.175 g, 0.83 mmol/g) were placed in five Teflon filter vessels. Fmoc deprotection with 20% piperidine−DMF (3 mL, 2×10 min) was followed by washing with DMF (2×). The appropriate carboxylic acid (5 equiv), HOBt (5 equiv), and DIC (5 equiv) in dry DMF (3 mL) were mixed together and after 15 min added to the resins, which were agitated at room temperature for 16 h. The resins were then drained and washed with DMF, MeOH, DMF, and CH_2Cl_2 (each 3×). Cleavage of the products from the resin was performed with 50% TFA−CH_2Cl_2 (5 mL for 2 h). The resins were washed with CH_2Cl_2 and MeOH (each 2 × 5 mL), and the combined eluates were concentrated in vacuo, coevaporated with toluene and MeOH (each 3 × 5 mL), and the residue was dried overnight. Purification of the crude material by preparative HPLC (using a linear gradient rising from 5% of B to 100% of B during 20 min) afforded **7**−**11** as the tris(TFA) salts. Compounds **9** and **10** required rechromatography (using a linear gradient rising from 5% B to 60% B during 20 min) to obtain sufficient purity.

Compound 7. Yield: 59 mg (54%); t_R = 15.13 min (99.8% at 220 nm). HRMS: calcd for $C_{23}H_{45}N_5O_2$ $[M + H]^+$ 424.36460, found 424.36444. ^{1}H NMR (300 MHz, CD_3OD): δ 4.25 (1H, dd, J = 8.8 and 6.3 Hz, H-α), 3.40−3.21 (2H, br m, H-1), 3.17−2.96 (10H, br m, H-3, H-4, H-7, H-8 and H-10), 2.09 (2H, m, H-9), 1.87 (2H, p, J = 6.6 Hz, H-2), 1.84−1.64 (10H, br m, cHex H_{eq}, H-5, H-6, and H-2′), 1.59 (2H, m, H-β), 1.40 (1H, m, H-γ), 1.34−1.14 (3H, br m, cHex H_{ax}), 1.05−0.88 (2H, br m, cHex H_{ax}), 0.86−0.76 (4H, br m, H-3′). ^{13}C NMR (75 MHz, CD_3OD): δ 176.7, 176.5, 53.3, 48.2, 48.1, 46.1, 45.8, 40.4, 37.8, 36.7, 35.4, 34.9, 33.4, 27.6 (2C), 27.4, 27.2, 25.4, 24.3 (2C), 14.6, 7.7 (2C).

Compound 8. Yield: 56 mg (48%); t_R = 17.78 min (>99.9% at 210 nm). HRMS: calcd for $C_{26}H_{51}N_5O_2$ $[M + H]^+$ 466.41165, found 466.41141. ^{1}H NMR (300 MHz, CD_3OD): δ 4.23 (1H, dd, J = 8.8 and 6.3 Hz, H-α), 3.39−3.23 (2H, br m, H-1), 3.16−2.96 (10H, br m, H-3, H-4, H-7, H-8, and H-10), 2.29 (1H, m, H-2′), 2.08 (2H, m, H-9), 1.86 (2H, p, J = 6.8 Hz, H-2), 1.84−1.64 (14H, br m, cHex H_{eq}, H-5, and H-6), 1.57 (2H, m, H-β), 1.50−1.13 (9H, br m, H-γ and cHex H_{ax}), 1.02−0.82 (2H, br m, cHex H_{ax}). ^{13}C NMR (75 MHz, CD_3OD): δ 179.4, 176.5, 52.9, 48.2, 48.1, 46.1, 45.9 (2C), 40.2, 37.8, 36.7, 35.5, 34.9, 33.2, 31.2, 30.3, 27.6 (2C), 27.4, 27.3, 26.9 (2C), 26.6, 25.4, 24.3 (2C).

Compound 9. Yield: 60 mg (48%); t_R = 19.75 min (>99.9% at 220 nm). HRMS: calcd for $C_{32}H_{49}N_5O_2$ $[M + H]^+$ 536.39590, found 536.39593. ^{1}H NMR (300 MHz, CD_3OD): δ 7.98 (2H, d, J = 8.8 Hz, BiPh ArH), 7.75 (2H, d, J = 8.8 Hz, BiPh ArH), 7.68 (2H, br d, J = 7.2 Hz, BiPh Ph), 7.47 (2H, br t, J = 7.2 Hz, BiPh Ph), 7.38 (1H, br t, J = 7.2 Hz, BiPh Ph), 4.52 (1H, dd, J = 10.1 and 5.4 Hz, H-α), 3.47−3.25 (2H, br m, H-1), 3.10−2.96 (10H, br m, H-3, H-4, H-7, H-8, and H-10), 2.05 (2H, m, H-9), 1.91 (2H, p, J = 6.7 Hz, H-2), 1.87−1.64 (11H, br m, H-β, cHex H_{eq}, H-5 and H-6), 1.47 (1H, m, H-γ), 1.38−1.16 (3H, br m, cHex H_{ax}), 1.14−0.90 (2H, br m, cHex H_{ax}). ^{13}C NMR (75 MHz, CD_3OD): δ 176.5, 170.0, 145.7, 140.9, 133.6, 129.5 (2C), 129.1 (3C), 128.0 (2C), 127.9 (2C), 53.9, 48.2, 48.1, 46.1, 45.8, 40.1, 37.7, 36.8, 35.7, 34.8, 33.4, 27.6 (2C), 27.4, 27.3, 25.4, 24.3 (2C).

Compound 10. Yield: 54 mg (44%); t_R = 18.53 min (>99.9% at 220 nm). HRMS: calcd for $C_{31}H_{49}N_5O_2$ $[M + H]^+$ 524.39590, found 524.39593. ^{1}H NMR (300 MHz, CD_3OD): δ 8.07 (1H, m, ArH), 7.91−7.79 (2H, br m, ArH), 7.57−7.43 (4H, br m, ArH), 4.24 (1H, dd, J = 9.6 and 5.5 Hz, H-α), 4.07 (2H, m, −CH_2=Ar), 3.39−3.18 (2H, br m, H-1), 3.09−2.70 (10H, br m, H-3, H-4, H-7, H-8, and H-10), 2.04 (2H, m, H-9), 1.79 (2H, p, J = 6.7 Hz, H-2), 1.72−1.50 (11H, br m, H-β, cHex H_{eq}, H-5 and H-6), 1.34−0.76 (6H, br m, H-γ and cHex H_{ax}). ^{13}C NMR (75 MHz, CD_3OD): δ 176.1, 174.1, 135.2, 133.4, 133.0, 129.7, 129.1, 128.8, 127.3, 126.8, 126.5, 125.0, 53.4, 48.2, 47.9, 46.0, 45.8, 41.0, 40.0, 37.8, 36.7, 35.3, 34.9, 33.1, 27.5 (2C), 27.4, 27.1, 25.4, 24.2, 24.1.

Compound 11. Yield: 54 mg (42%); t_R = 19.59 min (99.5% at 220 nm). HRMS: calcd for $C_{31}H_{57}N_5O_2$ $[M + H]^+$ 532.45850, found 532.45845. ^{1}H NMR (300 MHz, CD_3OD): δ 4.26 (1H, dd, J = 10.3 and 5.1 Hz, H-α), 3.38−3.24 (2H, br m, H-1), 3.16−2.97 (10H, br m, H-3, H-4, H-7, H-8, and H-10), 2.10 (2H, m, H-9), 2.08−1.91 (5H, br m, CH_2-Adm and Adm-H), 1.87 (2H, p, J = 6.9 Hz, H-2), 1.84−1.48 (23H, br m, H-β, cHex H_{eq}, H-5, H-6, and Adm-H), 1.43 (1H, m, H-γ), 1.34−1.10 (3H, br m, cHex H_{ax}), 1.06−0.83 (2H, br m, cHex H_{ax}). ^{13}C NMR (75 MHz, CD_3OD): δ 176.4, 174.0, 52.8, 51.6, 48.2, 48.1, 46.2, 45.8, 43.8 (3C), 39.9, 37.9 (3C), 37.8, 36.8, 35.3, 35.0, 34.0, 32.8, 30.2 (3C), 27.6 (3C), 27.3, 25.4, 24.4, 24.3.

SPS of Philanthotoxin Analogues containing Diamino Acid Residues. General Procedure E. In a syringe (20 mL, fitted with a filter and valve), 2-chlorotrityl chloride resin (2.38 g, 1.55 mmol/g) was swelled in dry CH_2Cl_2. Upon draining, the resin was treated with 10% iPr$_2$EtN in CH_2Cl_2 for 5 min and was then washed with CH_2Cl_2 (2 × 5 min). A solution of H_2N-$(CH_2)_3$NBoc$(CH_2)_4$NBoc$(CH_2)_3$NHTeoc[24] (2.22 g, 1.1 × 3.69 mmol) and iPr$_2$EtN (3.2 mL, 5 × 3.69 mmol) in CH_2Cl_2 (25 mL) was added to the resin in a round-bottom flask (50 mL). The suspension was stirred gently for 2 days. The resin was transferred to the syringe and washed with CH_2Cl_2 (2 × 15 mL, each 5 min). Capping of unreacted linker groups was performed with iPr$_2$EtN−MeOH−CH_2Cl_2 (5:15:80, 2 × 15 mL, each 3 min). The product was then dried overnight to yield the loaded resin (3.78 g, 74%, 0.73 mmol/g). In a round-bottomed flask (100 mL), Teoc-deprotection was performed with Bu_4NF (4.66 g, 5.3 equiv) in dry DMF (50 mL) at 50 °C for 1 h and then at room temperature for 4 h. The resin was transferred to the syringe, drained. and washed with DMF, MeOH, DMF, and CH_2Cl_2 (each 3×), and then dried overnight to yield resin **27** (3.53 g, 0.78 mmol/g).

Batches of the resin (200 mg, 0.156 mmol) in Teflon filter vessels were preswollen in DMF (5 mL) for 15 min and then drained. Protected diamino acid building block (**18**, **19**, **20**, or **21**, 3 equiv) in DMF (3 mL) was mixed with DIC (3 equiv) and HOBt (3 equiv) in dry DMF (3 mL), and after 15 min the solution was added to the resin and the suspension was agitated at room temperature for 16 h. The resin was drained and washed with MeOH and DMF (each 3 × 5 mL for 5 min), and then Fmoc deprotection was performed with 20% piperidine−DMF (3 mL, 2 × 10 min), followed by washing with DMF (5×). The resin was drained and dried (oil pump) for 16 h. Cyclohexanecarboxylic acid (3 equiv), HOBt (3 equiv), and DIC (3 equiv) in dry DMF (3 mL) were added to the resin, and the suspension was agitated at room temperature for 16 h. Upon draining and washing with DMF (5×), the Teoc group was removed by treatment with Bu_4NF (3 equiv) in dry DMF (6 mL) at 50 °C for 1 h followed by 2 h at room temperature. The resin was drained and washed with DMF, MeOH, DMF, and CH_2Cl_2 (each 3×). $PhCH_2COOH$ (3 equiv), HOBt (3 equiv), and DIC (3 equiv) in dry DMF (6 mL) were added, and then the mixture was agitated at room temperature for 16 h. The resin was washed with DMF, MeOH, DMF, and CH_2Cl_2 (3×), and cleavage was performed with 20% TFA in CH_2Cl_2 (3 mL for 30 min followed by 2 × 3 mL for 15 min). The resin was washed with CH_2Cl_2 and MeOH (each 2.5 mL) and the combined eluates were concentrated in vacuo, and the residue was coevaporated successively with MeOH and toluene (each 3 × 2.5 mL) and freeze-dried for 16 h. Purification of the crude by preparative HPLC (using a linear gradient rising from 5% of B to 100% of B during 20 min) afforded **12**−**15** as the tris(TFA) salts.

Compound 12. Yield: 110 mg (61%); t_R = 15.02 min (98.0% at 220 nm). HRMS: calcd for $C_{28}H_{48}N_6O_3$ $[M + H]^+$ 517.38607, found 517.38594. ^{1}H NMR (300 MHz, CD_3OD): δ 7.35−7.22 (5H, br m, Ph), 4.30 (1H, t, J = 6.3 Hz, H-α), 3.54 (2H, d, J = 6.3 Hz, H-β), 3.52 (2H, s, Ph-CH_2−), 3.27 (2H, br t, J = 6.5 Hz, H-1), 3.16−2.91 (10H, br m, H-3, H-4, H-7, H-8 and H-10), 2.17 (1H, m, cHex −CH <), 2.08 (2H, m, H-9), 1.87−1.64 (11H, br m, cHex H_{eq}, H-2, H-5 and H-6), 1.40−1.16 (5H, br m, cHex H_{ax}). ^{13}C NMR (75 MHz, CD_3OD): δ 179.2, 174.9, 173.3, 136.5, 130.1 (2C), 129.5 (2C), 127.9, 55.8, 48.2, 48.0, 46.1, 46.0, 45.8, 43.7, 41.6, 37.8, 36.8, 30.7, 30.3, 27.4, 26.9, 26.8, 26.7, 25.4, 24.3, 24.2.

Compound 13. Yield: 144 mg (78%); t_R = 15.07 min (98.7% at 220 nm). HRMS: calcd for $C_{29}H_{50}N_6O_3$ $[M + H]^+$ 531.40172, found 531.40173. ^{1}H NMR (300 MHz, CD_3OD): δ 7.34−7.20 (5H, br m, Ph), 4.17 (1H, dd, J = 8.2 and 5.9 Hz, H-α), 3.51 (2H, s, Ph-CH_2−), 3.34−3.16 (4H, br m, H-γ, H-1), 3.15−2.94 (10H, br m, H-3, H-4, H-7, H-8 and H-10), 2.27 (1H, m, cHex −CH <), 2.08 (2H, m, H-9), 2.01−1.89 (2H, br m, H-β), 1.89−1.65 (11H, br m, cHex H_{eq}, H-2, H-5 and H-6), 1.48−1.15 (5H, br m, cHex H_{ax}). ^{13}C NMR (75 MHz, CD_3OD): δ 179.4, 175.1, 174.2, 136.7, 130.0 (2C), 129.5 (2C), 127.8, 53.1, 48.2, 48.1, 46.2, 45.9, 45.8, 43.8, 37.8, 37.4, 36.8, 32.5, 30.9, 30.4, 27.6, 26.9, 26.8, 26.7, 25.4, 24.3, 24.2.

Compound 14. Yield: 128 mg (68%); t_R = 15.07 min (99.5% at 220 nm). HRMS: calcd for $C_{30}H_{52}N_6O_3$ $[M + H]^+$ 545.41737, found 545.41735. ^{1}H NMR (300 MHz, CD_3OD): δ 7.35−7.21 (5H, br m, Ph), 4.16 (1H, dd, J = 8.2 and 5.6 Hz, H-α), 3.50 (2H, s, Ph-CH_2−), 3.34−3.18 (4H, br m, H-δ and H-1), 3.17−2.93 (10H, br m, H-3, H-4, H-7, H-8 and H-10), 2.28 (1H, m, cHex −CH <), 2.09 (2H, m, H-9), 1.90−1.50 (15H, br m, H-β, H-γ, cHex H_{eq}, H-2, H-5 and H-6), 1.49−1.15 (5H, br m, cHex H_{ax}). ^{13}C NMR (75 MHz, CD_3OD): δ 179.4, 175.6, 174.1, 136.9, 129.9 (2C), 129.5 (2C), 127.8, 54.9, 48.2, 48.1, 46.1, 45.9, 45.8, 43.9, 39.9, 37.8, 36.7, 31.0, 30.4, 30.0, 27.6, 27.1, 26.9, 26.8, 26.7, 25.4, 24.3, 24.2.

Compound 15. Yield: 122 mg (64%); t_R = 15.53 min (98.2% at 220 nm). HRMS: calcd for $C_{31}H_{54}N_6O_3$ $[M + H]^+$ 559.43302, found 559.43291. ^{1}H NMR (300 MHz, CD_3OD): δ 7.33−7.19 (5H, br m, Ph), 4.08 (1H, dd, J = 8.7 and 5.7 Hz, H-α), 3.49 (2H, s, Ph-CH_2−), 3.35−3.23 (2H, br m, H-1), 3.18 (2H, t, J = 6.8 Hz, H-ε), 3.15−2.95 (10H, br m, H-3, H-4, H-7, H-8 and H-10), 2.28 (1H, m, cHex −CH <), 2.08 (2H, m, H-9), 1.90−1.60 (13H, br m, H-β, cHex H_{eq}, H-2, H-5 and H-6), 1.52 (2H, m, H-δ), 1.48−1.15 (7H, br m, H-γ and cHex H_{ax}). ^{13}C NMR (75 MHz, CD_3OD): δ 179.3, 175.8, 173.8, 136.9, 129.9 (2C), 129.5 (2C), 127.8, 55.3, 48.2, 48.1, 46.1, 45.8 (2C), 43.9, 40.1, 37.8, 36.7, 32.3, 31.0, 30.4, 30.0, 27.6, 26.9, 26.8, 26.7, 25.4, 24.4, 24.3, 24.2.

In Vitro cRNA Transcription. The cDNA encoding rat $GluA1_i$ or GluN1/2A subunits were inserted into the vectors pGEM-HE or pCIneo, respectively, for preparation of high-expression cRNA transcripts. Plasmids were grown in Top10 *Escherichia. coli* bacteria (Invitrogen, Carlsbad, CA) and isolated by using column purification (Qiagen, La Jolla, CA). The cRNA was synthesized from the above cDNAs by in vitro transcription using the mMESSAGE mMACHINE T7 mRNA-capping kit (Ambion, Austin, TX) according to the protocol supplied by the manufacturer.

Oocyte Electrophysiology. Mature female *Xenopus laevis* (Nasco, Modesto, CA) were anaesthetized using 0.1% ethyl 3-aminobenzoate, and their ovaries were surgically removed. The ovarian tissue was dissected and treated with collagenase in Ca^{2+}-free Barth's medium (2 mg/mL) for 1−2 h at room temperature. On the second day, oocytes were injected with 25 nL of cRNA (1 ng/nL of $GluA1_i$ or 0.05 ng/nL of GluN1 and GluN2A) and incubated at 17 °C in Barth's medium (in mM: 88 NaCl, 1 KCl, 0.33 $Ca(NO_3)_2$, 0.41 $CaCl_2$, 0.82 $MgSO_4$, 2.4 $NaHCO_3$, 10 HEPES; pH 7.4) with gentamicin (0.10 mg/mL). Oocytes were used for recordings 3−6 days postinjection and were voltage-clamped with the use of a two-electrode voltage clamp (Dagan Corporation, Minneapolis, MN) with both microelectrodes filled with 3 M KCl. Recordings were made while the oocytes were continuously superfused with frog Ringer's solution (in mM: 115 NaCl, 2 KCl, 1.8 $BaCl_2$, 5 HEPES; pH 7.6). The test compounds were dissolved in frog Ringer's solution and added by bath application. Recordings were performed at room temperature at holding potentials in the range from −80 to −40 mV. Antagonist concentration−response curves were constructed by measuring the maximal current induced by the saturating concentration of agonist (100 μM glutamate for $GluA1_i$; 100 μM glutamate and 100 μM glycine for GluN1/2A) and then applying increasing concentrations of antagonist in the presence of the appropriate agonist. Data from individual oocytes were fitted to the equation: $I = I_{max}/[1 + 10^{(\log IC_{50} - \log[\text{antagonist}])n_H}]$, where I is the response observed at a given antagonist concentration and I_{max} is the response in the absence of antagonist. The parameters I_{max} (maximal current observed at infinite agonist concentration), n_H (Hill coefficient), and the IC_{50} (concentration of antagonist producing 50% of I_{max}) were determined by an iterative least-squares fitting routine. Concentration−response curves were determined in triplicate for 3−8 individual oocytes. Statistical differences were analyzed using ANOVA followed by a Dunnett's multiple comparison test; * and ** denotes a levels of significance of $p < 0.05$ and $p < 0.01$, respectively.

References

(1) Blennow, K.; de Leon, M. J.; Zetterberg, H. Alzheimer's disease. *Lancet* **2006**, *368*, 387–403.
(2) Querfurth, H. W.; LaFerla, F. M. Alzheimer's disease. *N. Eng. J. Med.* **2010**, *262*, 329–344.
(3) Citron, M. Alzheimer's disease: strategies for disease modification. *Nature Rev. Drug Discovery* **2010**, *9*, 387–398.
(4) Lleo, A.; Greenberg, S. M.; Growdon, J. H. Current pharmacotherapy for Alzheimer's disease. *Ann. Rev. Med.* **2006**, *57*, 513–533.
(5) Schliebs, R.; Arendt, T. The significance of the cholinergic system in the brain during aging and in Alzheimer's disease. *J. Neural Transm.* **2006**, *113*, 1625–1644.
(6) Munoz-Torrero, D. Acetylcholinesterase inhibitors as disease-modifying therapies for Alzheimer's disease. *Curr. Med. Chem.* **2008**, *15*, 2433–2455.
(7) Lipton, S. A. Paradigm shift in neuroprotection by NMDA receptor blockade: memantine and beyond. *Nature Rev. Drug Discovery* **2006**, *6*, 160–170.
(8) Parsons, C. G.; Stoffler, A.; Danysz, W. Memantine: a NMDA receptor antagonist that improves memory by restoration of homeostasis in the glutamatergic system—too little activation is bad, too much is even worse. *Neuropharmacology* **2007**, *53*, 699–723.
(9) McKeage, K. Memantine, a review of its use in moderate to severe Alzheimer's disease. *CNS Drugs* **2009**, *23*, 881–897.
(10) Van Marum, R. J. Update on the use of memantine in Alzheimer's disease. *Neuropsychiatr. Dis. Treat.* **2009**, *5*, 237–247.
(11) Strømgaard, K.; Jensen, L. S.; Vogensen, S. B. Polyamine toxins: development of selective ligands for ionotropic receptors. *Toxicon* **2005**, *45*, 249–254.
(12) Eldefrawi, A. T.; Eldefrawi, M. E.; Konno, K.; Mansour, N. A.; Nakanishi, K.; Oltz, E.; Usherwood, P. N. Structure and synthesis of a potent glutamate receptor antagonist in wasp venom. *Proc. Natl. Acad. Sci. U.S.A.* **1988**, *85*, 4910–4913.
(13) Dingledine, R.; Borges, K.; Bowie, D.; Traynelis, S. F. The glutamate receptor ion channels. *Pharmacol. Rev.* **1999**, *51*, 7–61.
(14) Wollmuth, L.; Sobolevsky, A. Structure and gating of the glutamate receptor ion channel. *Trends Neurosci.* **2004**, *27*, 321–328.
(15) Mayer, M. Glutamate receptors at atomic resolution. *Nature* **2006**, *440*, 456–462.
(16) Strømgaard, K.; Brier, T. J.; Andersen, K.; Mellor, I. R.; Saghyan, A.; Tikhonov, D.; Usherwood, P. N. R.; Krogsgaard-Larsen, P.; Jaroszewski, J. W. Solid-phase synthesis and biological evaluation of a combinatorial library of philanthotoxin analogues. *J. Med. Chem.* **2000**, *43*, 4526–4533.
(17) Chhabra, S. R.; Khan, A. N.; Bycroft, B. W. Solid-phase synthesis of polyamines using a Dde-linker: philanthotoxin-4.3.3 via an on-resin Mitsunobu reaction. *Tetrahedron Lett.* **2000**, *41*, 1099–1102.
(18) Strømgaard, K.; Andersen, K.; Ruhland, T.; Krogsgaard-Larsen, P.; Jaroszewski, J. W. A versatile method for solid-phase synthesis of polyamines: neuroactive polyamine toxins as example. *Synthesis* **2001**, 877–884.

(19) Kan, T.; Kobayashi, H.; Fukuyama, T. Highly versatile synthesis of polyamines by Ns-strategy on a novel trityl chloride resin. *Synlett* **2002**, 1338–1340.
(20) Andersen, T. F.; Strømgaard, K. Synthesis of Polyamine Toxins. An improved alkylation procedure. *Tetrahedron Lett*. **2004**, *45*, 7929–7933.
(21) Olsen, C. A.; Witt, M.; Jaroszewski, J. W.; Franzyk, H. Diols as building blocks in solid-phase synthesis of polyamine toxins by Fukuyama−Mitsunobu alkylation. *Synlett* **2004**, 473–476.
(22) Olsen, C. A.; Witt, M.; Jaroszewski, J. W.; Franzyk, H. Solid-phase synthesis of rigid acylpolyamines using temporary *N*-4,4′-dimethoxytrityl protection in the presence of trityl linkers. *J. Org. Chem*. **2004**, *69*, 6149–6152.
(23) Jørgensen, M. R.; Jaroszewski, J. W.; Witt, M.; Franzyk, H. On-resin carboxy group activation of ω-amino acids in solid-phase synthesis of philanthotoxin analogues. *Synthesis* **2005**, 2687–2694.
(24) Olsen, C. A.; Franzyk, H.; Jaroszewski, J. W. *N*-Alkylation reactions and indirect formation of amino functionalities in solid-phase synthesis. *Synthesis* **2005**, 2631–2653.
(25) Wellendorph, P.; Jaroszewski, J. W.; Hansen, S. H.; Franzyk, H. A sequential high-yielding large-scale solution-method for synthesis of philanthotoxin analogues. *Eur. J. Med. Chem*. **2003**, *38*, 117–122.
(26) Olsen, C. A.; Mellor, I. R.; Wellendorph, P.; Usherwood, P. N. R.; Witt, M.; Franzyk, H.; Jaroszewski, J. W. Tuning wasp toxin structure for nicotinic receptor antagonism: cyclohexylalanine-containing analogues as potent and voltage-dependent blockers. *ChemMedChem* **2006**, *1*, 303–305.
(27) Jørgensen, M. R.; Olsen, C. A.; Mellor, I. R.; Usherwood, P. N. R.; Witt, M.; Jaroszewski, J. W.; Franzyk, H. The effects of conformational constraints and steric bulk in the amino acid moiety of philanthotoxins on AMPAR antagonism. *J. Med. Chem*. **2005**, *48*, 56–70.
(28) Olsen, C. A.; Jørgensen, M. R.; Hansen, S. H.; Witt, M.; Jaroszewski, J. W.; Franzyk, H. Side-chain-anchored N^{α}-Fmoc-Tyr-OPfp for bidirectional solid-phase synthesis. *Org. Lett*. **2005**, *7*, 1703–1706.
(29) Strømgaard, K.; Brierley, M. J.; Andersen, K.; Sløk, F. A; Mellor, I. R.; Usherwood, P. N. R.; Krogsgaard-Larsen, P.; Jaroszewski, J. W. Analogues of neuroactive polyamine wasp toxins that lack inner basic sites exhibit enhanced antagonism toward a muscle-type mammalian nicotinic acetylcholine receptor. *J. Med. Chem*. **1999**, *42*, 5224–5234.
(30) Kromann, H.; Krikstolaityte, S.; Andersen, A. J.; Andersen, K.; Krogsgaard-Larsen, P.; Jaroszewski, J. W.; Egebjerg, J.; Strømgaard, K. Solid-phase synthesis of polyamine toxin analogues: potent and selective antagonists of Ca^{2+}-permeable AMPA receptors. *J. Med. Chem*. **2002**, *45*, 5745–5754.
(31) Jaroszewski, J. W.; Matzen, L.; Frølund, B.; Krogsgaard-Larsen, P. Neuroactive polyamine wasp toxins: nuclear magnetic resonance spectroscopic studies of the protolytic properties of philanthotoxin-343. *J. Med. Chem*. **1996**, *39*, 515–521.
(32) Strømgaard, K.; Piazzi, L.; Olsen, C. A.; Franzyk, H.; Jaroszewski, J. W. Protolytic properties of polyamine wasp toxin analogues studied by ^{13}C NMR spectroscopy. *Magn. Reson. Chem*. **2006**, *44*, 1013–1022.
(33) Kallimopoulos, R.; Bukownik, K.; Nakanishi, P.; Usherwood, A.; Eldefrawi, A.; Eldefrawi, M. Structure−activity relationships of philanthotoxin analogs and polyamines on *N*-methyl-D-aspartate and nicotinic acetylcholine receptors. *J. Pharmacol. Exp. Ther*. **1990**, *254*, 764–773.
(34) Olsen, C. A.; Witt, M.; Franzyk, H.; Jaroszewski, J. W. Solid-phase synthesis of neuroactive spider−wasp hybrid toxin analogues using a backbone amide linker. *Tetrahedron Lett*. **2007**, *48*, 405–408.
(35) Nelson, J. K.; Frølund, S. U.; Tikhonov, D. B.; Kristensen, A. S.; Strømgaard, K. Synthesis and biology of argiotoxin-636 and analogues: selective antagonists for ionotropic glutamate receptors. *Angew. Chem., Int. Ed*. **2009**, *49*, 3087–3091.
(36) Drake, B.; Patek, M.; Lebl, M. A convenient preparation of monosubstituted *N*,*N*′-di(Boc)-protected guanidines. *Synthesis* **1994**, 579–582.
(37) Bonke, G.; Vedel, L.; Witt, M.; Jaroszewski, J. W.; Olsen, C. A.; Franzyk, H. Dimeric building blocks for solid-phase synthesis of α-peptide−β-peptoid chimeras. *Synthesis* **2008**, 2381–2390.
(38) Rosowsky, A.; Wright, J. E. N^{ϵ}-[[2-Trimethylsilyl)ethoxy]carbonyl] derivatives of tri-L-lysine and tetra-L-lysine as potential intermediates in the block polymer synthesis of macromolecular drug conjugates. *J. Org. Chem*. **1989**, *54*, 5551–5558.
(39) Ha, S.; Chang, E.; Lo, M.-C.; Men, H.; Park, P.; Ge, M.; Walker, S. The kinetic characterization of *Escherichia coli* MurG using synthetic substrate analogues. *J. Am. Chem. Soc*. **1999**, *121*, 8415–8426.
(40) Bresink, I.; Benke, T. A.; Collett, V. J.; Seal, A. J.; Parsons, C. G.; Henley, J. M.; Collingridge, G. L. Effects of memantine on recombinant rat NMDA receptors expressed in HEK 293 cells. *Br. J. Pharmacol*. **1996**, *119*, 195–204.
(41) Gilling, K. E.; Jatzke, C.; Hechenberger, M.; Parsons, C. G. Potency, voltage-dependency, agonist concentration-dependency, blocking kinetics and partial untrapping of the uncompetitive *N*-methyl-D-aspartate (NMDA) channel blocker memantine at human NMDA (GluN1/GluN2A) receptors. *Neuropharmacology* **2009**, *56*, 866–875.
(42) Dravid, S. M.; Erreger, K.; Yuan, H.; Nicholson, K.; Le, P.; Lyuboslavsky, P.; Almonte, A.; Murray, E.; Mosely, C.; Barber, J.; French, A.; Balster, R.; Murray, T. F.; Traynelis, S. F. Subunit-specific mechanisms and proton sensitivity of NMDA receptor channel block. *J. Physiol*. **2007**, *581*, 107–128.